



Changes in the thermoelectric power of a Ni base superalloy induced by elastic and plastic strain

E. López Cuéllar^{a,b,*}, E. Reyes Melo^{a,b}, A. Martínez-de la Cruz^{a,b}, A. García Loera^{a,b}, M. Morin^c

^a Posgrado de FIME, Universidad Autónoma de Nuevo León, A.P. 076 Suc. "F", Cd. Universitaria C.P. 66450, San Nicolás de los Garza, N.L., Mexico

^b CIIDIT, Universidad Autónoma de Nuevo León, Avenida Alianza 101 Sur parque PIIT Monterrey, Apodaca, N.L. 66600, Mexico

^c MATEIS, UMR CNRS 5510, INSA de Lyon, Bât. Blaise Pascal, 7 av. Jean Capelle, F-69621 Villeurbanne, France

ARTICLE INFO

Article history:

Received 21 September 2010

Received in revised form 15 April 2011

Accepted 19 April 2011

Available online 27 April 2011

Keywords:

Thermoelectric

Strain

Elasticity

Mechanical properties

Alloys

ABSTRACT

Induced changes in the thermoelectric power (TEP) of the Inconel 718 by elastic and plastic strain have been previously reported by López Cuéllar et al. [1]. Now, in this work, the TEP of a nickel-based superalloy Waspaloy with different heat treatments has been followed during stressing tests. In all cases plastic deformation has been attained. TEP measurement variations of ~ 160 nV/°C have been attained for a certain heat treatment that produces the desirable γ' phase, and low changes of TEP are observed for the treatment that does not produce γ' . Like for the Inconel 718, results indicate that TEP of the Waspaloy is clearly affected by the elastic and plastic strain induced during tests. The previously proposed model to describe the change in TEP induced by the strain in specimens of Inconel 718 [1], is validated with the Waspaloy superalloy in this work. Thus, these results confirm that the TEP technique is a powerful tool to detect non-desirable states and levels of strain in alloys containing γ' phase like the Waspaloy and Inconel superalloys.

© 2011 Elsevier B.V. All rights reserved.

1. Introduction

Waspaloy is an age hardenable nickel base super alloy that possesses high temperature strength (≈ 980 °C) with a good corrosion resistance, especially to oxidation. In this nickel-based superalloy, the matrix (γ phase) is hardened by γ' particles and by a small amount of MC and $M_{23}C_6$ carbides. The chemical composition of the Waspaloy [2] is as follows (wt%): Cr 11.4, Co 14.0, Mo 4.5, Fe 0.6, Al 1.22, Ti 3.13, C 0.033, B 0.005, Ni bal. The amount of Al and Ti leads to a γ' volume fraction of about 25%. The Cr, Co, and Mo elements cause an additional solid solution hardening with a low tendency to form topological-closed packed phases after long-time service. Nowadays, Waspaloy is often encountered in extreme environments. It is common in gas turbine blades, seals, rings, shafts and turbine disks. However a disadvantage of this material is the tendency to form macrosegregations during the solidification after remelting, called freckles, which influences the castability in a negative way. This fact can lead to the development of cracks during the subsequent forging process. Another negative effect on the forgeability is the fast precipitation of γ' at forging temperatures, which increases the forging forces required. In this sense, in a recent work

it has been reported that the thermoelectric power (TEP) for a Ni-base superalloy (Inconel 718), is sensitive to non-desirable phase and is clearly affected by the elastic and plastic strain induced during tests [1,3]. In consequence, the TEP characterization technique can be considered useful to follow elastic and plastic strain, and for the study of residual stress in the Inconel 718 alloy. The TEP technique can be considered as a non-destructive characterization technique depending of the equipment arrangement [4,5]. TEP effect is achieved when two junctions of two metals are brought to two different temperatures; then an electromotive force appears between these two junctions [6]. This electromotive force is characteristic of each different junction of metals and for some alloys. Moreover, it has been shown that if the microstructure or composition is modified, the TEP of this junction will also change. For this reason, the TEP technique is currently used to finely characterize any microstructural evolution of metallic materials [7]. For example, the percentage of cold work and the recrystallised grain size have been followed by TEP variations of the Austenitic stainless steels AISI 304 [7]. It has been shown that the change of the Seebeck coefficient has the potential for non-destructive monitoring of the neutron embrittlement of RPV steels [8]. The temperature of the austenite to martensite phase transition in the ferromagnetic shape memory alloy $Ni_{50}Mn_{34}In_{16}$ has been associated with a sharp change in the TEP and the thermal conductivity curves of the alloy [9]. TEP has proven to be an excellent tool to evaluate the carbon and nitrogen content in iron and steels [10–13], the critical temperature for the Fe_3Al was marked by a sharp change in the slope

* Corresponding author at: Posgrado de FIME, Universidad Autónoma de Nuevo León, A.P. 076 Suc. "F", Cd. Universitaria C.P. 66450, San Nicolás de los Garza, N.L., Mexico. Tel.: +52 81 83294020; fax: +52 81 83320904.

E-mail address: lopezcuellar@gama.fime.uanl.mx (E. López Cuéllar).

of TEP vs. temperature plot and the phase boundary was also determined [14]. The TEP detected the dissolution of $M_{23}C_6$ carbides in an X45Cr13 stainless steel [12]. TEP was a good method to evaluate thermal aging, possibly caused by the concentration of Cr in a cast duplex stainless steel [13]. Finally, recrystallisation and precipitation processes were studied with this technique in the alloy 8011 Al–Fe–Si [15].

In this work, the mechanical behaviour during tensile tests of several heat treatments with and without the desirable γ' phase of the Waspaloy alloy was studied by following the material's Δ TEP. For this purpose, a special tensile machine that allows the stress and strain control during TEP measurements was utilized [1]. Samples with γ' has shown important Δ TEP, attaining ~ 160 nV/ $^\circ$ C for higher strain levels, while samples without γ' has shown lower variations of ~ 20 nV/ $^\circ$ C. Moreover, like for the Inconel, Δ TEP of samples with γ' phase, have shown a strong lineal behaviour with elastic and plastic strains, which is a very interesting result from the point of view of determination of material's residual stress and plastic deformation. Finally, the lineal model previously reported [1], that predicts the TEP behaviour during tensile tests, is validated with the Waspaloy system, presenting also a statistical analysis of the variation between the experimental results and the expected values from the model.

2. Experimentation

The Waspaloy alloy was provided by the company Frisa Aerospace. Samples were obtained from an aero engine turbine component at the forging stage and the initial thermomechanical treatment was also carried out by the ring mill. To avoid important microstructural changes, samples were cut by Electrical Discharge Machining with dimensions of 1 mm \times 0.5 mm \times 100 mm. After the machining process, several heat treatments were done in a Nabertherm (B-150) furnace, see Table 1. In order to induce different microstructural states, the TTT Diagrams and heat treatments (HT) proposed by Penkalla et al. [2] were carried out. To clear the as-received state, samples were heat treated at 1100 $^\circ$ C during 1 h and cooled in water (HT A) or air (HT B), in both cases, a state without γ' phase was expected. Contrary, heat treatments C, D and E were done in the aim to induce the development of the γ' phase (see Table 1).

TEP and strain tests were done simultaneously with special equipment designed by Morin in the MATEIS laboratory. This mechanical test machine (MTM) was previously described [1] and allows to measure the sample's TEP, strain and stress during tensile tests. TEP measurements were obtained with a TEP Techlab PK120 with Copper blocks. To avoid electrical contact between the mechanical test machine and the TEP blocks, a sandpaper insulator was used between the sample and machine jaws. During the mechanical tests, TEP blocks do not apply pressure on the sample, i.e., they are not in contact with the sample. After applying certain level of stress, the motor of the MTM stops, maintaining a constant stress on the sample. After that, TEP blocks get contact with the sample with two pneumatic pistons at a constant pressure. The TEP measurements were done, when practically no variation of TEP values were detected in the computer and the value is the average of at least 20 measurements. Finally, TEP values were obtained during charging and discharging the sample.

The first cycle was done just before the yield strength of each state was reached. For the second cycle the level of applied stress was increased and so on. The process of the cycles was carried out until reaching the failure of the material or the MTM limits.

3. Results and discussion

Fig. 1 indicates the results of stress vs. strain of all heat treatments reported in Table 1. As expected, HT A shows the lower value of strength ($\sigma_Y < 400$ MPa), indicating that the microstructure is free

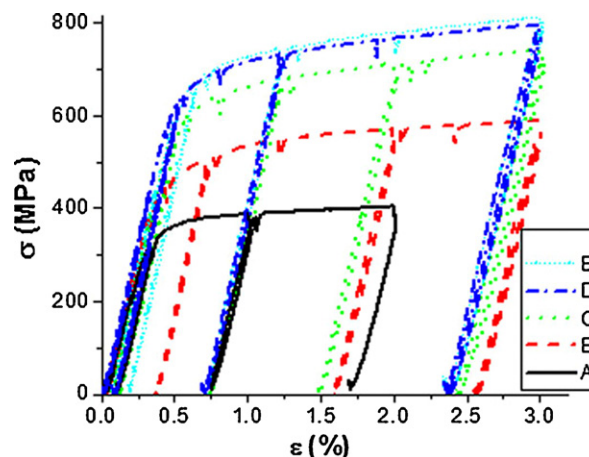


Fig. 1. Results of stress vs. strain for Waspaloy samples with A, B, C, D, and E heat treatments.

of the γ' phase. However, when the cooling rate is decreased by changing the cooling fluid from water to air as in HT B, an important increase of strength is observed ($\sigma_Y > 500$ MPa). According to the TTT Diagram proposed by Penkalla et al. [2], a free microstructure of the γ' phase was also expected, but probably because the cooling fluid is the air at room temperature, HT B process gives some time to start the formation of some γ' phase, increasing the strength. For HT C, D and E an increase of the strength ($\sigma_Y > 600$ MPa) is clearly observed due to the γ' phase. It is well known that the γ' phase has a crystal ordered cell L12 [16,17] and this order gives to the superalloys, an increase in their mechanical properties, which is in agreement with these results. Another feature can be observed in Fig. 1 is that results show little steps in the curve, decreasing the stress at the time of the TEP measurements. These steps are caused when TEP blocks are brought together with the sample with the two pneumatic pistons.

Fig. 2(a and b) shows the data of Δ TEP at a given applied stress (σ) and strain (ϵ) for all heat treatments and number of cycles respectively. As can be seen in Fig. 2(a), a decrease in the material's TEP takes place in all cases when the sample is stressed, but a different clear behaviour is present between HT A and all the other HT. While HT A does not show a correlation, HT B to HT E show a lineal correlation between Δ TEP and σ . A similar behaviour but with a greater apparent dispersion in the experimental data is observed from Δ TEP vs. ϵ results as can be seen in Fig. 2(b). Finally, two important effects can be appreciated in this Fig. 2(b), first when the period of time of the HT is increased the Δ TEP are lower and second, HT A shows a higher dispersion. A clear observation of this phenomenon can be appreciated in Fig. 3, where only results of Δ TEP vs. ϵ of HT C and A are plotted. If the behaviour of Δ TEP vs. ϵ of HT C is compared with the σ vs. ϵ behaviour of Fig. 1, a strong similitude can be found, but contrary; no relation can be found for the HT A.

These results suggest that the TEP of the samples with HT B to HT E are clearly dependent of the applied stress and the induced strain on the sample. On the other hand, the TEP of HT A, where no γ' phase is expected, cannot be related with the stress and the strain. This effect was observed before by López Cuéllar et al. [1,3] in the Inconel 718 alloy, and it was attributed to the atomic position order found in crystal structures of γ' and γ'' and the absent atomic order of γ respectively. Moreover, the Δ TEP of HT B to HT E seem to be affected proportionally during the elastic and plastic zones. Anisotropic effects on TEP have been reported in other materials [4,18].

Then, supported in the observations done above in the samples with HT B to HT E, it was possible to extract from the experimental

Table 1
Heat treatments and expected phases from Penkalla et al. [2].

State	Heat treatment	Expected phases
A	1100 $^\circ$ C-1 h, water cooled	γ
B	1100 $^\circ$ C-1 h, air cooled	γ
C	After B, 850 $^\circ$ C-2 h, water cooled	$\gamma + \gamma' + MC$
D	After B + C, 760 $^\circ$ C-3 h, water cooled	$\gamma + \gamma' + MC$
E	After B + C, 760 $^\circ$ C-15 h, water cooled	$\gamma + \gamma' + MC$

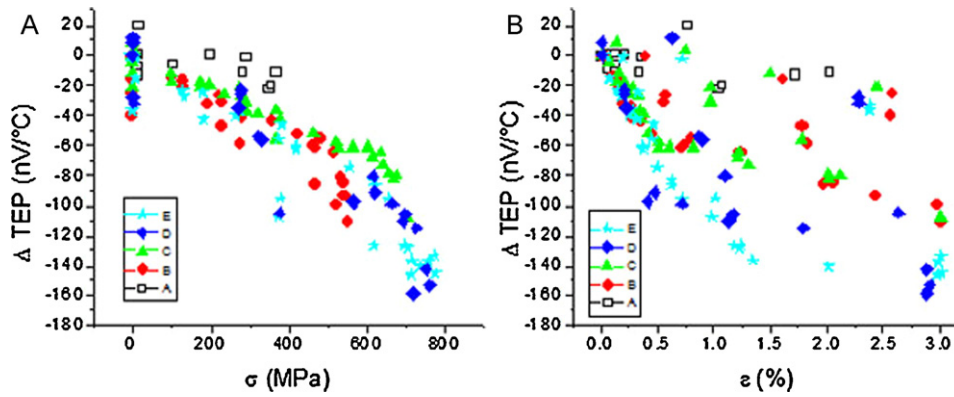


Fig. 2. (a) ΔTEP vs. σ results for all HT samples. (b) ΔTEP vs. ϵ for all HT samples.

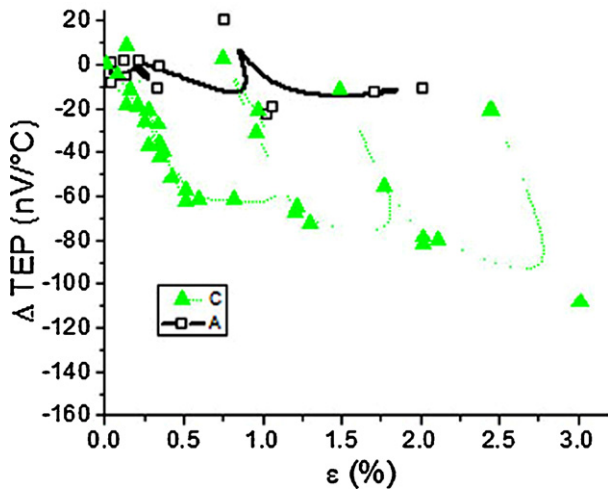


Fig. 3. ΔTEP vs. σ results only for C and A HT samples.

results the contribution of the plasticity and the elasticity on the material's TEP. These contributions are plotted in Fig. 4(a and b) respectively. First, the contribution of plasticity can be calculated at the end of the unloading for each cycle and each HT, i.e. with 0MPa, because at this step of the tensile test of stress, the permanent effect on the material is only the plastic strain, in this way this first assumption is justified. A lineal contribution of the plasticity was obtained from Fig. 4(a) and is reported in Table 2.

To isolate the elastic contribution, the lineal contribution of plastic deformation reported in Table 2 was subtracted from the

Table 2

Lineal contribution of plasticity and elasticity on TEP material.

State	Plastic contribution $\Delta S/\epsilon_p$ (nV/°C/% ϵ_p)	Elastic contribution $\Delta S/\epsilon_{el}$ (nV/°C/% ϵ_{el})
B	-12.15	-170.28
C	-9.63	-147.75
D	-16.12	-209.94
E	-13.29	-187.86

unloading results of each HT. As can be seen in Fig. 4(b), even the results with high values of strain are aligned with all other values between 0 and 0.7% for all the HT. Then a lineal contribution from Fig. 4(b) of elasticity was calculated for each HT and reported in Table 2.

Now, to follow the behaviour of TEP during the deformation of the Waspaloy samples with HT B to E, the same model used before for the Inconel 718 alloy [1] is applied in this work. The expected model is illustrated in Fig. 5(a and b) and is built with Eqs. (1)–(3). Eq. (1) describes the elastic behaviour during loading the sample. Once elasticity achieves the lost of linear ratio σ/ϵ , the plastic deformation starts to act in the material and ϵ_p gets into the calculus as described in Eq. (2). Eq. (3) describes the behaviour during unloading the sample, here only the elastic component is taken into account.

$$\Delta TEP_{el\ load} = \frac{\Delta S}{\epsilon_{el}} \times \epsilon \tag{1}$$

$$\Delta TEP_{pl\ load} = C_1 + \frac{\Delta S}{\epsilon_p} \times \epsilon \tag{2}$$

$$\Delta TEP_{el\ unload} = C_1 + C_2 - \frac{\Delta S}{\epsilon_{el}} \times \epsilon \tag{3}$$

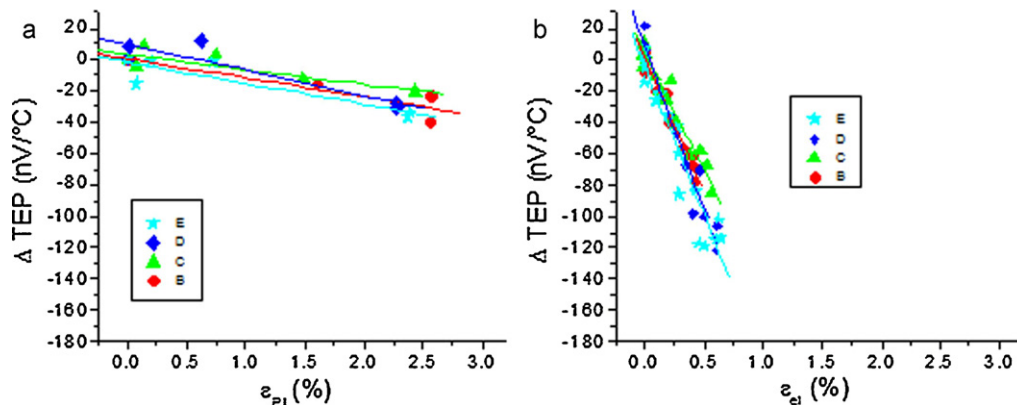


Fig. 4. (a) Contribution of the plastic strain (ϵ_p) on the TEP material for B, C, D, and E HT samples obtained from data shown in Fig. 2(b). (b) Results of ΔTEP vs. ϵ_{el} during unloading the sample subtracting the contribution of plastic strain ϵ_p .

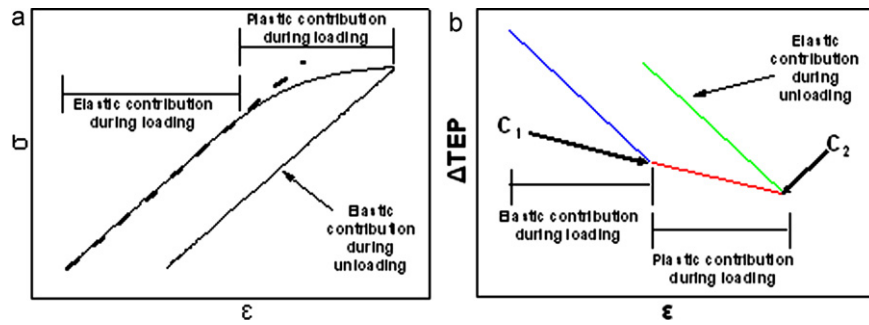


Fig. 5. (a) The different zones of elastic contribution (ε) from one σ vs. ε schema and (b) from one ΔTEP vs. ε schema.

where $\Delta TEP_{el\ load}$ is the change in material TEP induced by the elastic strain during loading the sample, $\Delta S/\varepsilon_{el}$ is the contribution of the elasticity on the TEP reported in Table 2, ε is the experimental strain of the material during the tensile test, $\Delta TEP_{pl\ load}$ is the change in material TEP induced by the plastic strain during loading the sample, C_1 is a constant when elasticity achieves the loss of lineal ratio σ/ε and the material begins to deform plastically, $\Delta S/\varepsilon_p$ is the contribution of the plasticity on the TEP reported in Table 2, $\Delta TEP_{el\ unload}$ is the change in material TEP induced by the elastic strain during unloading the sample, C_2 is the second constant defined at the end of the sample loading. In this way, knowing the strain induced in the alloy, the behaviour of ΔTEP during a cycle of tensile test can be predicted.

Now, if the experimental strain results reported in Fig. 1 are introduced in Eqs. (1)–(3), respecting the outlined zones of Fig. 5 for each equation, a complete loading–unloading cycle can be constructed for each HT in the Waspaloy samples, as is shown in Fig. 6(a–d). The predicted values of ΔTEP with the model during loading are indicated in blue (elastic contribution) and red (plastic contribution) respectively, and during unloading in green (elastic

contribution). Experimental values of TEP are plotted with solid symbols. As can be appreciated, the values obtained from the model for each HT are very close to the experimental results.

From experimental and theoretical results shown in Fig. 6 a statistical analysis was carried out in order to validate the model for the Waspaloy superalloy. For this, the absolute value of the difference between the experimental (ER) and model results (EM) was calculated ($|ER-EM|$) at the same level of strain for each experimental result obtained. In general, for all HT most of the differences are lower than 12 nV/°C. Fig. 7(a–d) shows the histograms (frequency vs. the bin end of the $|ER-EM|$) obtained for HT B to E respectively. From this figure it can be observed that the more accurate HT was the B, i.e. values of bin end are closer to zero, but also for this HT is founded the lower ΔTEP as a function of the strain, for example ΔTEP is ~ 95 nV/°C when ε is 3% (Fig. 6(a)). As the HT increases for HT C to E, this accuracy decreases ($|ER-EM|$ increases), but ΔTEP is ~ 140 nV/°C when ε is also 3% for HT E (Fig. 6(d)). This suggests that this accuracy will proportionally decrease when $\Delta TEP/\varepsilon$ increases. This behaviour could be associated to the limit of linear behaviour of $\Delta TEP=f(\varepsilon)$.

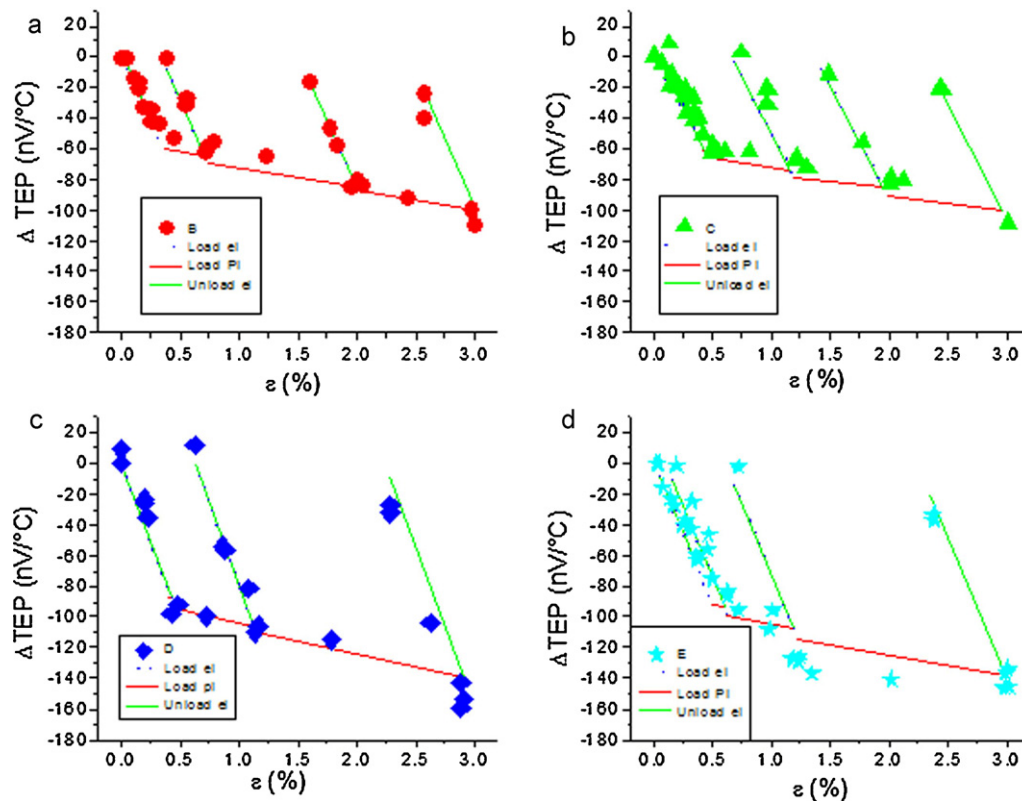


Fig. 6. (a–d) Comparison between the values of DTPE predicted with the model (continuous lines) and experimental measurements obtained during loading.

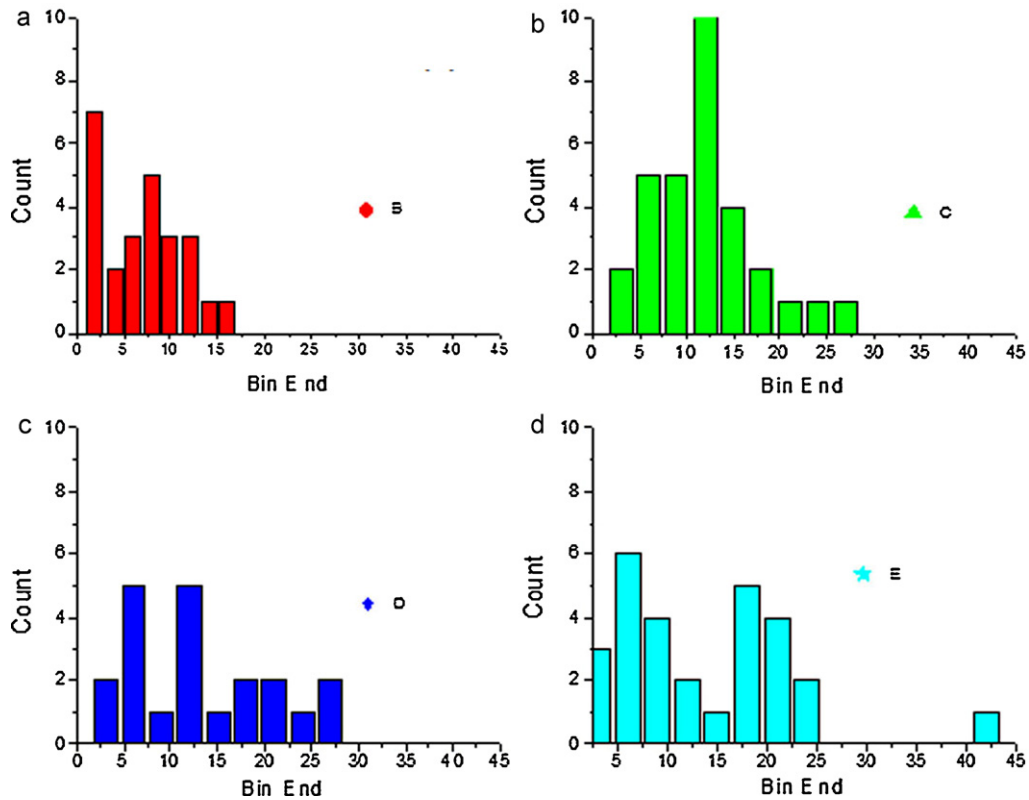


Fig. 7. (a–d) The histograms (frequency vs. the bin end of |ER-EM|) obtained from Fig. 6a–d, corresponding to HT B to E respectively.

Of course, in this work a lineal relationship is proposed to make a faster and easier analysis of results, but because of plasticity there is a high possibility that the relation of TEP with ε will not be lineal. In this sense, to propose a more complex model, a statistical analysis using more samples must be done. Despite the model simplicity, from the application point of view, with this model seems to be possible to predict the level of strain if the Δ TEP for the Waspaloy is known or to predict the Δ TEP when the alloy is deformed. This could be a very attractive application in the aerospace industry if these experiments are carried out with an in situ TEP apparatus, like the apparatus used by Carreon [4], leading to a non-destructive test of characterization of pieces under service, providing valuable information that could save huge amount of costs due to reprocessing of distorted parts.

Finally, experimental values of Δ TEP for the Waspaloy at 3% of ε have attained ~ 160 nV/°C for certain HT, while for the Inconel only ~ 24 nV/°C at 2.2% of ε [1]. This seems to indicate that the TEP of γ' founded in the Waspaloy is more affected with the strain than the TEP of γ'' mostly founded in the Inconel system. To elucidate this, future works must be done with other superalloys: one only with γ' phase (Rene 41), and a second one only with γ'' phase (Inconel 706).

4. Conclusions

For Waspaloy samples without γ' phase (HT A), the lowest value of strength ($\sigma_y < 400$ MPa) is obtained. For samples with HT B, C, D, and E an increase of the strength ($\sigma_y > 500$ MPa) is clearly observed due to the presence of γ' phase.

The TEP of the material presents also two different behaviours: the Δ TEP of HT B, C, D and E shows a strong dependence of the strain, while no correlation is observed between the Δ TEP of HT A and the strain. This dependence of the material's TEP of the HT seems to be associated to the presence of the γ' phase, so,

this must be attributed to the FCC ($L1_2$) structure present in this phase. The induced strain in the crystal cells with an atomic order position must cause a change in the free electron path when the Seebeck effect is created; other anisotropic phenomena have been related with changes in material's TEP. The same lineal model previously reported for the Inconel 718 [1] was validated in this work with samples of Waspaloy at different HT. This model that predicts the TEP changes induced by the strain has been developed deconvoluting the Δ TEP caused by the plastic strain at 0 MPa from measurements during the sample unloading. In this model, the material's Δ TEP is lineal dependent of the elastic and plastic strain. Different relationships between Δ TEP and strain have been found for each HT, which certainly can be attributed to the amount of γ' developed during heat treatments. TEP characterization technique can be considered useful to follow elastic and plastic strains in the Waspaloy system when γ' phase is present; the desirable phase for the alloy's application in aerospace industry. Moreover these results have proven that TEP can be used to study residual stress of the alloy.

Acknowledgments

The authors would like to acknowledge the financial support from the CONACYT of México for the project J39554-Y and 82515. And also authors would like to acknowledge the technical support from all the staff of the MATEIS laboratory and PhD Hugo Guajardo from FRISA Aerospace.

References

- [1] E. López Cuéllar, M. Morin, E. Reyes Melo, U. Ortiz Méndez, H. Guajardo Martínez, J. Yerena Cortéz, J. Alloys Compd. 467 (2009) 572–577.
- [2] H.J. Penkalla, J. Wosik, A. Czyrska-Filemonowicz, Mater. Chem. Phys. 81 (2003) 417–423.

- [3] E. López Cuéllar, L. López Pavón, U. Ortiz Méndez, E. Reyes Melo, A. Martínez de la Cruz, M. Morin, H. Guajardo Martínez, *Advances in Condensed Matter and Materials Research*, vol. 8, Nova Science Publishers, 2011, ISBN 978-1-60876-159-3.
- [4] H. Carreon, *NDT & E Int.* 39 (6) (2006) 433–440.
- [5] K. Yasuhiro, Y. Shinsuke, *Jpn. Inst. Met.* 66 (4) (2002) 377–383.
- [6] X. Kleber, L. Simonet, F. Fouquet, M. Delnondedieu, *Mater. Sci. Eng.* 13 (2005) 341–354.
- [7] C. Capdevila, T. De Cock, F.G. Caballero, D. San Martin, C. Garcia de Andres, *J. Mater. Sci.* 44 (2009) 4499–4502.
- [8] M. Niffenegger, H.J. Leber, *J. Nucl. Mater.* 389 (2009) 62–67.
- [9] L.S. Sharath Chandra, M.K. Chattopadhyay, V.K. Sharma, S.B. Roy Sudhir, K. Pandey, *Phys. Rev. B* 81 (19) (2010), 195105-1-8.
- [10] V. Massardier, V.N. Lavaire, M. Soler, J. Merlin, *Scripta Mater.* 50 (2004) 1435–1439.
- [11] N.R. Borrelly, D. Benkirat, *Acta Metall.* 33 (1985) 855–866.
- [12] F.G. Caballero, C. Capdevila, L.F. Alvarez, C.G. de Andrés, *Scripta Mater.* 50 (2004) 1061–1066.
- [13] Y. Kawaguchi, S. Yamanaka, *J. Alloys Compd.* 336 (2002) 301–314.
- [14] G. Erez, P.S Rudman, *J. Phys. Chem.* 18 (1961) 307–315.
- [15] N.J.A. Luiggi, *Metall. Mater. Trans. A* 29A (1998) 2669–2677.
- [16] R.F. Decker, *J.O.M.* 58 (9) (2006) 32–36.
- [17] Sims, Stoloff, Hagel, *Superalloys II High-Temperature Materials for Aerospace and Industrial Power*, John Wiley & Sons, New Jersey, 1987.
- [18] E. López Cuéllar, G. Guénin, M. Morin, *Mater. Sci. Eng. A* 358 (2003) 350–355.